Biologically inspired design of hydrogel-capped hair sensors for enhanced underwater flow detection†

Michael E. McConney,[a] Nannan Chen,[b] David Lu,[a] Huan A. Hu,[b] Sheryl Coombs,[c] Chang Liu[b] and Vladimir V. Tsukruk*[a]

Received 28th May 2008, Accepted 28th August 2008
First published as an Advance Article on the web 22nd October 2008
DOI: 10.1039/b808839j

Using a precision drop-casting method, a bioinspired hydrogel-capped hair sensory system was created, which enhanced the performance of flow detection by about two orders of magnitude and endowed the sensors with threshold sensitivities that rival those of fish.

Biologically inspired design is a problem solving approach, which often results in unique engineered solutions.[1,2] There are many examples of successful applications, such as infrared imagers based on viper pit organs and forest-fire searching beetles,[3,4] materials capable of legless locomotion inspired by the anisotropic friction of snake locomotion,[5] mimicking flow sensitive hair structures,[6] and the ability to defy gravity by walking on walls inspired by the setae of geckos.[7]

The hair cells of vertebrates are particularly interesting from a bioinspired design standpoint due to their amazing sensitivity (displacement sensitivity in the nm range) and their functional versatility. For example, hair cells in the lateral line system of fish are capable of detecting water flows past the body surface with velocities of a few micron per second.[8] This functional versatility is made possible by the variety of specialized auxiliary structures that mechanically link sound, body motions or surrounding flows to the ciliary bundles of the hair cells. Such structures include membranes, bones, otolithic masses, fluid-filled canals, and gelatinous structures known as cupulae. Fish have been shown to use the flow sensing hair cells of their lateral line for a variety of important functions, including prey localization, predator avoidance, and schooling.[9] As such, the lateral line system serves as bioinspiration for the engineered development of flow sensing abilities in autonomous underwater vehicles, including the ability to detect hydrodynamic disturbances created by moving bodies and stationary bodies in a flow field, to manoeuvre effectively in complex turbulent flow conditions and minimize drag and increase locomotion efficiency.[10]

In this regard, the blind cave fish, *Astyanax fasciatus* provides an ideal model system for inspiring engineered flow sensors, because these fish have evolved under dark conditions that favored the development and reliance on flow sensing receptors (Fig. 1a–c). Because their eyes have degenerated, these fish form hydrodynamic rather than visual images of their surrounding environment. As they glide past stationary objects, they can detect the obstacle-created distortions in their own self-generated flow field. The hydrodynamic imaging abilities of blind cavefish allow them to avoid collision with nearby obstacles[11] and to make fine spatial discriminations of the order of 1 mm.[12] The lateral line system of blind cavefish, as well as other species, consists of many, spatially-distributed flow sensors, called neuromasts (Fig. 1b).

Neuromasts can be divided into two basic categories—those directly on the skin surface (superficial neuromasts) and those in fluid-filled canals just under the skin surface. Blind cavefish have several anatomical specializations of the lateral line system, which include superficial neuromasts with greater cross-sectional areas and taller cupulae. Although superficial neuromasts tend to be smaller (<100 um in diameter) and have fewer hair cells than canal neuromasts in all species, the two classes of receptors are similar in their basic anatomy and basic flow sensing function. The cupula of superficial neuromasts tend to have high aspect ratios, such that the distal end of the cupula is outside the boundary layer, exposed to the free stream region of the flow field, and bent (Fig. 1c and d).[13]

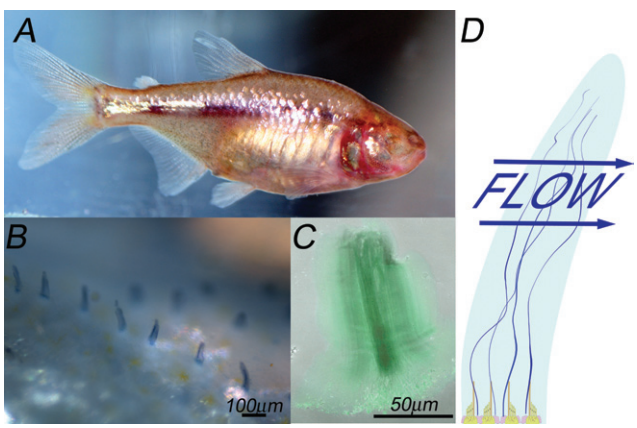

Fig. 1 (A) The blind cave fish evolved in darkness and relies on flow receptors for "imaging", instead of eyesight. (B) An optical micrograph showing a row of stained cupulae within a lateral line. (C) A confocal image of a single cupula. (D) Schematic of the neuromast structure that shows how the bent cupula couples the underlying hair receptors to the surrounding flow.

[a]*School of Materials Science and Engineering, School of Polymer, Textile, and Fiber Engineering, Georgia Institute of Technology, Atlanta, GA, 30332, USA. E-mail: Vladimir@mse.gatech.edu; Fax: +1 (1) 404 385 3112; Tel: +1 (1) 404 894 6081*
[b]*Department of Electrical Engineering, University of Illinois at Urbana-Champagne, Urbana, IL, 61801, USA*
[c]*Department of Biological Sciences, JP Scott Center for Neuroscience, Mind & Behavior, Bowling Green State University, Bowling Green, OH, 43403, USA*

† Electronic supplementary information (ESI) available: Comparative sensitivity data for two independent sensors; cupula deposition on an actual sensor at 1000× speed. See DOI: 10.1039/b808839j

These different flow sensing structures are thought to be designed to sense different aspects of the surrounding fluidic flow: constant velocity distribution and fluid acceleration distribution, allowing for reconstruction of the full picture of the underwater surrounding.

Here we report, bioinspired flow sensors in which the engineered hair sensor has been covered with a compliant hydrogel structure coming from morphological lessons of the superficial neuromasts discussed above.[14] The work presented here significantly expands a previously reported study involving the development of a bio-inspired hydrogel material with a low aspect ratio (height to diameter ratio close to 1:1) and relatively high elastic modulus (10 kPa) thus biomimicking the "sliding" mechanism of flow detection with canal neuromasts.[14] In contrast, the current study focuses on hydrogels with a modulus of the order of 10 Pa, in order to better replicate the inherent properties of the biological *superficial cupula* with its "bending" mechanism of flow detection. Furthermore, in this study we also developed a method to recreate the high aspect ratio structure (aspect ratio reaching 5:1) observed in biological superficial cupula. This work serves as an essential stepping stone in developing a synthetic analog of the high aspect ratio superficial cupula of the fish hence completing a set of sensors for both velocity and acceleration sensing of surrounding flow down to extremely low values (almost stationary water). By creating higher aspect ratio very compliant structures capable of sensing beyond the boundary layer (Fig. 1d), we were able to impart sensing abilities to the flow sensors rivalling those of fish.

Having successfully developed a polymer that can mimic the cupula material earlier, we set out to mimic the high aspect ratio cupula in superficial receptors to further improve the sensors' capabilities. The height and width of blind cave fish superficial cupula were studied with conventional optical microscopy and confocal fluorescence microscopy. Only superficial cupula with circular footprints were analyzed and studies were focused on the superficial neuromasts along the opercle. Confocal fluorescence microscopy was used for an initial detailed study of the morphology and dimensions of the cupula, whereas optical microscopy was used to analyze the dimensions of many cupula and generate representative statistics. For imaging cupulae of blind cavefish superficial neuromasts, fish were first anesthetized and then dipped into a filtered 0.1% Janus green or methylene blue solution for 5 minutes to render cupulae visible under optical microscopy. The cupula involved in fluorescent confocal microscopy studies were further treated by removing them from the fish by suction with a small micropipette under a stereomicroscope. Cupulae were then placed in a 1 μg/ml solution, made from a 0.1% solution of 5-DTAF dissolved in DMSO for epifluorescent visualization. Because cupulae are pH-sensitive, all solutions were made from filtered aquarium water buffered to the same pH (~7.5) as the original aquarium water after the anesthetic or stains were added. From these studies, we concluded that the superficial cupula had a height of 104 ± 13 μm, a width of 26 ± 3 μm, and an aspect ratio of 4.0 ± 0.8 (see Fig. 1b and c).

A synthetic high aspect ratio hydrogel cupula was fabricated directly on a hair flow sensor by dispensing a specific volume of macromonomer solution precisely onto the hair without wetting the sensor platform (for sensor description see ref. 15). The poly(ethylene glycol) tetraacrylate (PEG-TA, M_w = 18 000, Polyscience, Inc) dissolved in methanol was prepared according to conditions described elsewhere.[14] A syringe with a solution attached to a 3-axis micro-positioning system equipped with a camera of the side-view was aligned in the horizontal plane over the hair (Fig. 2a). Then while the syringe was several hundred μm above the hair, a droplet of less than 1 μl was dispensed from the syringe tip. While the droplet was still hanging from the syringe tip, the syringe was slowly lowered onto and through the hair using the z-axis micrometer. The syringe diameter was significantly larger than the hair diameter, so with careful alignment, the syringe did not interfere with the hair. After the droplet made contact with the hair, the droplet was furthered lowered over the length of the hair. The methanol was allowed to partially evaporate for several seconds, until the droplet became slightly viscous and opaque, then the syringe was raised, leaving the droplet on the hair. The syringe was periodically raised several μm, essentially sliding the droplet back and forth along the hair until the droplet stayed on the hair. Once the droplet dried, then another droplet was lowered until it made contact with the last drop and it was deposited in the same manner to build a tall hydrogel structure. An example of the manufacturing routine can be seen in the movie file in the ESI.†

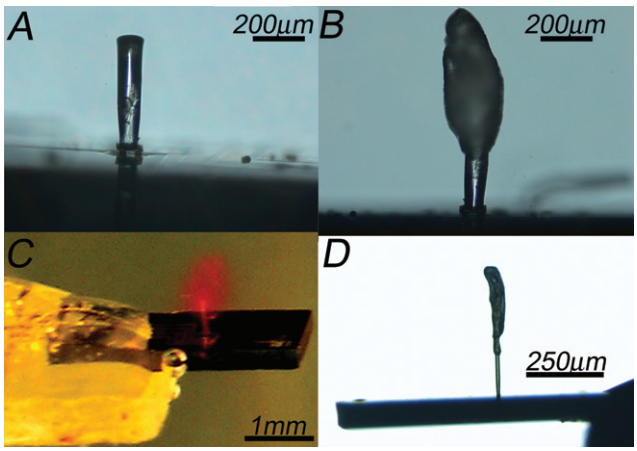

Fig. 2 The front-view of a hair sensor (A) before and (B) after being coated with the PEG-based hydrogel material. (C) A swollen cupula on a working sensor (the hydrogel is dyed using rhodamine). (D) The side-view of a sensor with a long SU-8 hair and a long/high aspect ratio cupula in the dry state.

This method allowed the synthetic cupula to be applied to the hair and built up, without wetting the base of the sensor, thereby leading to high aspect ratio structures (Fig. 2b–d). Furthermore, this method provides the ability to control the width and height of the cupula by controlling the dispensed volume of each droplet and by controlling the number of droplets, respectively. The distance from the bottom of the cupula to the base of the hair, can be also controlled. When the synthetic cupula was placed closest to the sensor platform the durability and lifetime of the cupula structure was enhanced. We found that depositing a cupula which started half-way up the hair and extended past the hair by about 50% was a good balance between robustness, height and preventing wetting of the platform. In the case of the few tested sensors, the microfabricated hairs were 550 μm long and the dried cupula started at about 275 μm above the base of the hair and ended about 275 μm above the hair, giving the total hair–dry cupula structure a height of roughly 825 μm (Fig. 2b). At this distance, wetting the platform was minimized and still the cupula remained intact for months. Furthermore, when the hydrogel cupula was allowed to swell, the base of the cupula nearly reached the sensor platform. The full process involved dropping about 10 droplets of

solution to form the desired height and width (see examples of two structures in Fig. 2b and d).

Once the dried synthetic cupula structure had formed, we cross-linked the functionalized PEG macromonomer by photoirradiating the sample with UV light (365 nm) for 6 minutes at an intensity of 1000 mW/cm^2. Under these conditions, hydrogel structures showed elastic moduli in the range 5–50 Pa as measured and discussed elsewhere.[16] After the samples were irradiated they were allowed to swell for 45 minutes in the water tank before measurements were performed.

The completely assembled hair sensors with hydrogel cupulae (cupulae are stained for visibility, Fig. 2c) were tested using a permanent magnet shaker that sinusoidally actuated a dipole with an embedded velocity sensor to measure the amplitude and frequency of the dipole movement (Fig. 3a). The sensors were mounted on a metal platform connected to a micrometer, which accurately controlled the distance of the sensor platform to the dipole, all elements were placed in a water tank mounted on an air table (Fig. 3b). The sensors were mounted such that the dipole moved perpendicular to the long axis of the hair. The "bare" sensors were tested at a distance of 15 mm away at a constant frequency of 50 Hz. At 15 mm, the dipole shaker is capable of producing a minimum flow velocity of 85 μm/s, which was below the sensing threshold for the "bare" sensor. After the addition of the cupula, the sensing threshold was much lower and therefore required moving the dipole 45 mm away to accommodate the sensing threshold.

The results of the test showed a dramatic improvement in flow sensitivity with the addition of the high aspect hydrogel cupula onto hair sensor (Fig. 4a). The signal output which is proportional to the hair deflection in fluid flow increases linearly with flow velocity but the overall slope is much higher for the modified sensor. Initially, the bare sensor had a velocity sensitivity of 1.2 nm/(mm/s) (nm hair deflection per mm/s flow velocity) and 3.2 mV/(mm/s) (sensor output per mm/s flow velocity) with maximum deflection reaching only 10 nm. After the addition of the hydrogel cupula the sensitivity increases

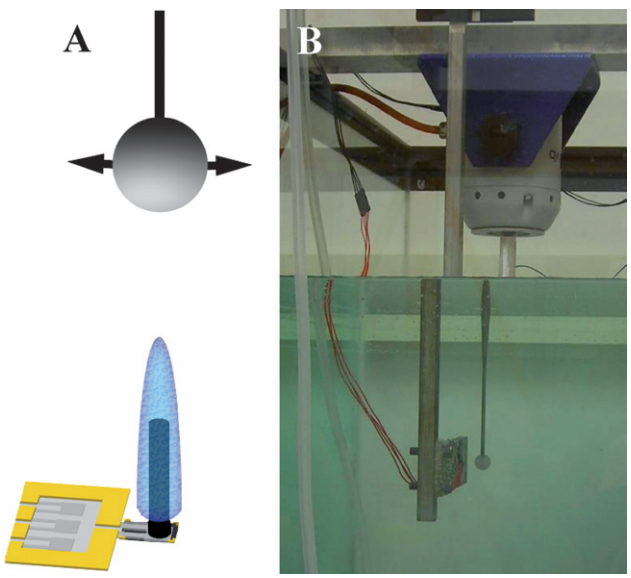

Fig. 3 (A and B) A permanent magnet shaker was positioned above the sensor and a sinusoidal frequency was applied while the displacement was measured with a sensor embedded inside the dipole.

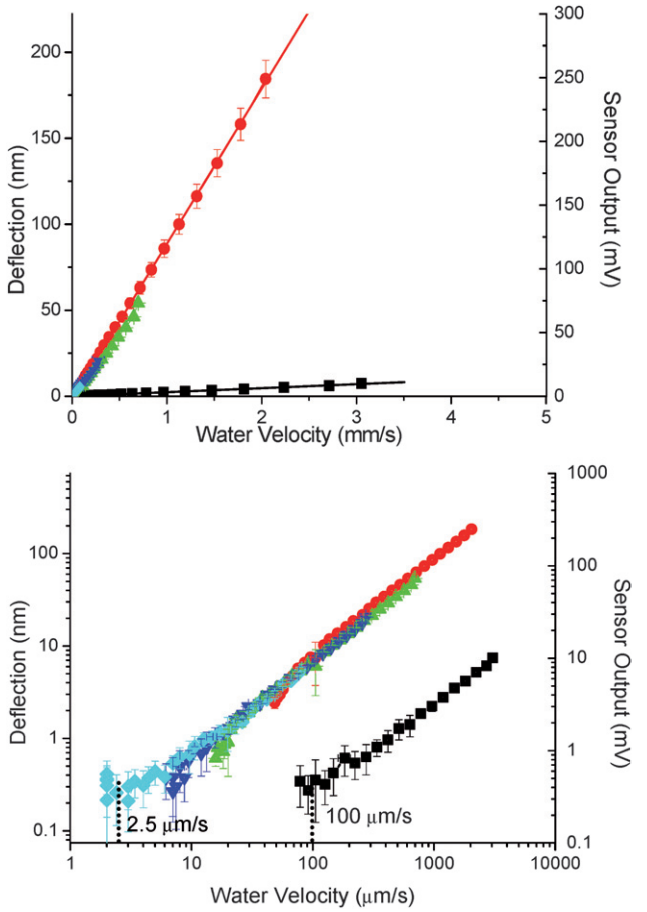

Fig. 4 (A) The results of the minimum threshold deflection measurements plotted on a linear scale, showing an improvement in the sensitivity of 40 times. (B) The results of the threshold deflection measurements plotted on a log–log scale, showing an improvement in the threshold deflection of 40 times. (A and B) Black squares: "bare" sensor response at 15 mm distance from the dipole; red circles, green triangles, dark blue triangles, light blue diamonds sensor response with cupula, 15 mm, 22 mm, 30 mm, 45 mm distances from the dipole, respectively. Errors bars represent deviation for repeatable measurements for the same distance and sensor.

to 45 nm/(mm/s) and 122 mV/(mm/s), an overall improvement of 38 times (Fig. 4a).

Moreover, the "bare" sensor had a minimum velocity threshold of 100 μm/s (defined by signal output equal to background noise), but after the sensor was coated with the high aspect ratio cupula the threshold was 2.5 μm/s, an improvement of 40 times (Fig. 4b). This improvement was very repeatable for different distances (Fig. 4b) and sensors. After coating a second sensor with a similar cupula the velocity sensitivity improvement was 36 times and the minimum threshold velocity was improved from 200 μm/s to 6 μm/s an overall improvement of 33 times (for comparison of two independent sensors see ESI†). Moreover, the improvement was consistently observed for a wide range of frequencies from 10 to 90 Hz tested here.

The best velocity sensitivity threshold of 2.5 μm/s achieved here is extremely low as compared to current available sensors and a biological example.[13] Estimates of velocity sensitivity threshold for fish flow receptors varies significantly, with those derived from AC signals being as low as 18–38 μm/s for the frequency range 10–20 Hz[8] and

those from unidirectional, DC flow to even above 1 cm/s.[17] The sensitivity threshold for a sensor encapsulated in a dome-like stiffer cupula reported earlier did not exceed 75 μm/s which is 30 times lower that the sensitivity demonstrated here. Therefore, the overall velocity sensitivity threshold achieved here by means of the addition of very compliant, high aspect ratio hydrogel cupula to hair sensors make them truly rival the performance of fish flow receptors.

Acknowledgements

The authors thank J. Humphrey for fluid dynamics discussions, S. Peleshanko and K. Anderson for help with optimizing the hydrogel solution, and M. Ornatska for her help with optical microscopy measurements. This work was supported by a grant from the Defense Advanced Research Projects Agency.

Notes and references

1 (*a*) Y. Bar-Cohen, *Biomimetics: Biologically Inspired Technologies*, CRC Press, Boca Raton, FL, 2006; (*b*) J. Yen and Marc Weissburg, Perspectives on Biologically Inspired Design: Introduction to the Collected Contributions, *Bioinsp. Biomim.*, 2007, 2.
2 V. V. Tsukruk, M. Ornatska and A. Sidorenko, *Progr. Organic Coatings*, 2003, **47**, 288–291.
3 (*a*) N. Fuchigami, J. Hazel, V. V. Gorbunov, M. Stone, M. Grace and V. V. Tsukruk, *Biomacromolecules*, 2001, **2**, 757–764; (*b*) C. Jiang, M. E. McConney, S. Singamaneni, E. Merrick, Y. Chen, J. Zhao, L. Zhang and V. V. Tsukruk, *Chem. Mater.*, 2006, **18**, 2632–2634; (*c*) V. Gorbunov, N. Fuchigami, M. Stone, M. Grace and V. V. Tsukruk, *Biomacromolecules*, 2002, **3**, 106–111.
4 J. Hazel, N. Fuchigami, V. Gorbunov, H. Schmitz, M. Stone and V. V. Tsukruk, *Biomacromolecules*, 2001, **2**, 304–310.
5 (*a*) J. Hazel, M. Stone, M. S. Grace and V. V. Tsukruk, *J. Biomech.*, 1999, **32**, 477–484; (*b*) L. Mahadevan, S. Daniel and M. K. Chaudhury, *P. Natl. Acad. USA*, 2004, **101**, 23–26.
6 C. Liu, *Bioinsp. Biomim.*, 2007, **2**, S162–S169.
7 (*a*) K. Autumn, Y. A. Liang, S. T. Hsieth, W. Zesch, W. P. Chan, T. W. Kenny, R. Fearing and R. J. Full, *Nature*, 2000, **405**, 681–685; (*b*) A. K. Geim, S. V. Dubonos, I. V. Griforievam, K. S. Novoselov, A. A. Zhukov and S. Y. Shapoval, *Nat. Mater.*, 2003, **2**, 461–463; (*c*) K. Autumn, M. Sitti, Y. A. Liang, A. M. Peattie, W. R. Hansen, S. Sponberg, T. W. Kenny, R. Feraring, J. N. Israelachvili and R. J. Full, *P. Natl. Acad. USA*, 2002, **99**, 12252–12256.
8 (*a*) A. B. A. Kroese, J. M. Van der Zalm and J. Van der Berken, *Pflug. Arch. Eur. J. Phy.*, 1978, **375**, 167–175; (*b*) (b)S. Coombs and J. Janssen, in *The Mechanosensory Lateral Line: Neurobiology and Evolution*, ed. S. Coombs, P. Görner and H. Münz, Springer-Verlag, NY, 1989, pp. 299–319.
9 S. Coombs and J. C. Montgomery, in *Comparative Hearing: Fishes and Amphibians*, ed. A. N. Popper and R. R. Fay, Springger-Verlag, New York, 1st edn, 1999, vol. 11, pp. 319–362.
10 S. Coombs, *Auton. Robot.*, 2001, **11**, 255–261.
11 T. Teyke, *J. Comp. Physiol. A*, 1985, **157**, 837–843.
12 E. Hassan, *J. Comp. Physiol. A*, 1986, **159**, 701–710.
13 M. J. McHenry and S. M. van Netten, *J. Exp. Biol.*, 2007, **210**, 4244–4253.
14 S. Peleshanko, M. D. Julian, M. Ornatska, M. E. McConney, M. C. LeMieux, N. Chen, C. Tucker, Y. Yang, C. Liu, J. A. C. Humphrey and V. V. Tsukruk, *Adv. Mater.*, 2007, **19**, 2903–2909.
15 C. Liu, *Adv. Mater.*, 2007, **19**, 3783–3790.
16 K. D. Anderson, D. Lu, M. McConney, T. Han, D. Reneker and V. V. Tsukruk, *Polymer*, DOI: 10.1016/j.polymer.2008.09.039.
17 (*a*) J. C. Montgomery, C. F. Baker and A. G. Carton, *Nature*, 1997, **389**, 960–963; (*b*) S. Coombs, R. R. Fay and J. Janssen, *J. Acoust. Soc. Am.*, 1989, **85**, 2185–2193.